THE JOURNAL OF PHYSICAL CHEMISTRY B

Article

pubs.acs.org/JPCB

Computational and Experimental Study of the Behavior of Cyano-Based Ionic Liquids in Aqueous Solution

Marta L. S. Batista,[†] Kiki A. Kurnia,[†] Simão P. Pinho,[‡] José R. B. Gomes,[†] and João A. P. Coutinho*,[†]

[†]Departamento de Química, CICECO, Universidade de Aveiro, 3810-193 Aveiro, Portugal

[‡]Associate Laboratory LSRE/LCM, Instituto Politécnico de Bragança, 5301-857 Bragança, Portugal

Supporting Information

ABSTRACT: The solvation of cyano- (CN-) based ionic liquids (ILs) and their capacity to establish hydrogen bonds (H-bonds) with water was studied by means of experimental and computational approaches. Experimentally, water activity data were measured for aqueous solutions of ILs based on 1-butyl-3-methylimidazolium ([BMIM]$^+$) cation combined with one of the following anions: thiocyanate ([SCN]$^-$), dicyanamide ([DCA]$^-$), or tricyanomethanide ([TCM]$^-$), and of 1-ethyl-3-methylimidazolium tetracyanoborate ([EMIM]-[TCB]). From the latter data, water activity coefficients were estimated showing that [BMIM][SCN] and [BMIM][DCA], unlike [BMIM][TCM] and [EMIM]-[TCB], are able to establish favorable interactions with water. Computationally, the conductor like screening model for real solvents (COSMO-RS) was used to estimate the water activity coefficients which compare well with the experimental ones. From the COSMO-RS results, it is suggested that the polarity of each ion composing the ILs has a strong effect on the solvation phenomena. Furthermore, classical molecular dynamics (MD) simulations were performed for obtaining an atomic level picture of the local molecular neighborhood of the different species. From the experimental and computational data it is showed that increasing the number of CN groups in the ILs' anions does not enhance their ability to establish H-bonds with water but decreases their polarities, being [BMIM][DCA] and [BMIM][SCN] the ones presenting higher propensity to interact.

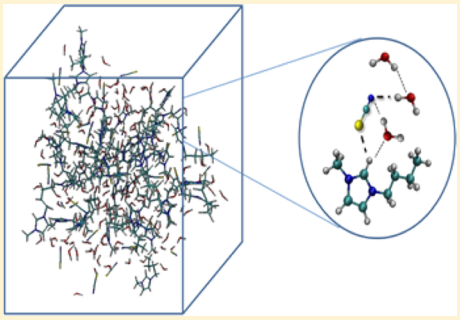

1. INTRODUCTION

Ionic liquids (ILs) are a new generation of solvents, composed of bulky organic cations and organic or inorganic anions that together create an asymmetric structure. This structuring disables their crystallization, and therefore, ILs are liquid at, or close to, room temperature. They present several unique properties. They present, in general, low vapor pressure, high chemical and thermal stabilities, and they are liquid in a wide range of temperatures and possess a good solvation capability that allows them to dissolve both polar and nonpolar compounds, as well as biopolymers, such as cellulose. Additionally, these properties can be tuned by changing the constituting cations and/or anions, which ultimately will enable the design of compounds with optimal characteristics for a specific application.[1]

It is well-known that the presence of water on ILs modifies their properties, such as viscosity[2,3] (lowering) or surface tension[4] (increasing) but also changes their structure and, above a given concentration, is capable of disrupting the ionic interaction between the cation and the anion.[5] The knowledge of the ILs' properties in aqueous solution is very important for their design and use in many applications namely, absorption refrigeration, extractive distillation or liquid−liquid extraction.[6,7] Furthermore, it is important to note that the ability of ILs to establish H-bonds with water, or other compounds, is related mainly with the nature of the anions, affecting not only their physical and chemical properties, but also their solvation potential, e.g., in the dissolution of carbohydrates.[8]

In the literature it is possible to find several experimental works based on infrared[9,10] (IR) and nuclear magnetic resonance[11,12] (NMR) spectroscopic techniques, or liquid−liquid equilibria[13,14] (LLE), vapor−liquid equilibria[15,16] (VLE), solid−liquid equilibria[17] (SLE), and activity coefficients[18] measurements that aimed careful characterization of water-IL systems. Moreover, theoretical approaches such as COSMO-RS[6,19,20] or classical MD[21−23] simulations have been also employed to complement the experimental studies and were found to provide important insights regarding the interactions involved in those systems. In addition, several review articles[1,5,24,25] reporting studies on binary systems composed of water and ILs by means of MD simulations were also published. Different factors governing the IL-water interactions, such as the nature of the cation, anion or combination of both, the cation's alkyl chain length, formation of aggregates and the dichotomy ion pairs vs isolated ions, were addressed in those studies. It is generally accepted that the anion predominantly establishes interactions with water and hence, the chemical nature of the anion assumes a pivotal role in the solvation of ILs.[9,25−27] Formation of water and/or IL aggregates is

Received: October 7, 2014
Revised: December 19, 2014
Published: December 22, 2014

DOI: 10.1021/jp510125x
J. Phys. Chem. B 2015, 119, 1567−1578

observed, and the composition at which it occurs is related with the nature/strength of the IL−water interactions. It is important to highlight that ILs have an unique structure, with microscopic domains, responsible for their high capability to dissolve a variety of compounds.[28] These domains are divided into two regions with polar and nonpolar character, with the latter being essentially formed by the cation's alkyl chains. In aqueous solution, these chains tend to aggregate into hydrophobic clusters, inducing similarly the formation of small clusters of water that, eventually, can become a homogeneous network, disrupting the cation−anion interactions. However, it should be noted that MD simulations are dependent on the accuracy of the applied force field, i.e., the bonded and nonbonded parameters or the applied atomic charges. From the latter, arises the question of the applicability of polarizable force fields which is currently a topic of discussion.[29] Therefore, it is important to develop force fields that can reproduce properties of ILs or mixtures containing ILs. In this regard, comparing the predicted physical properties, for example, density and viscosity, against experimental data, it can be assessed the general quality of the new developed force field. While densities of ILs are easily reproduced with short time computer simulations, longer time is required to obtain accurate viscosity values, due to their low dynamics/high viscosity. As it will be shown latter, densities calculated in this work are in good agreement with available experimental data.

Within the huge number of possible combinations between cations and anions, the CN-based ILs are interesting for industrial purposes because they present lower melting points and viscosities than most of ILs.[30] They have been studied and characterized for specific applications, mainly for electrolytes and dye-sensitized solar cells,[31,32] but also as extracting solvent for alcohols from fermentation broth,[33] for aromatic−aliphatic separation,[34] as well as for added-value compounds in biomass, such as phenolic compounds,[35] carbohydrates,[36,37] and sugar alcohols.[38] Recently, Neves et al.[30] published density and viscosity data for the pure imidazolium-based IL with CN-based anions, addressing the effect of the increase of the CN groups on these properties.

In the present work, binary systems composed of water and [BMIM][SCN], [BMIM][DCA], [BMIM][TCM], or [EMIM][TCB] were studied and characterized by means of experimental water activity data and computational approaches, namely COSMO-RS and MD simulation. It should be noted that [EMIM][TCB] was chosen due to the unavailability of [BMIM][TCB] from the supplier. Nevertheless, previous studies[9,39] showed that interactions between water and ILs are established mainly through the anion, while the imidazolium cation has a minor contribution. Thus, and for the first time, the set of CN-based ILs used in the present work, will allow us to study the effects of the number of CN groups in the anion, from 1 in $[SCN]^-$ to 4 in $[TCB]^-$, in the interaction of the ILs addressed in this work with water molecules.

As a reliable property to interpret such interactions, activity coefficients were estimated from water activity measurements for all these binary mixtures, at 298.2 K, which were further evaluated by COSMO-RS. Classical MD simulations were also performed to calculate the number of H-bonds given by coordination numbers, and also radial and spatial distribution functions for the different IL−water systems, from which information regarding the local atomic organization is evaluated.

2. EXPERIMENTAL SECTION

2.1. Materials. The ILs 1-butyl-3-methylimidazolium thiocyanate, [BMIM][SCN] (mass fraction purity >98%), 1-butyl-3-methylimidazolium dicyanamide, [BMIM][DCA] (mass fraction purity >98%), 1-butyl-3-methylimidazolium tricyanomethanide, [BMIM][TCM] (mass fraction purity >98%), were purchased from IoLiTec, while 1-ethyl-3-methylimidazolium tetracyanoborate, [EMIM][TCB] (mass fraction purity >98%) was kindly supplied by Merck KGaA Germany. Figure 1 depicts the chemical structures of the ions composing the studied ILs. The purities were further confirmed by ^1H and ^{13}C NMR and found to be in agreement with the purity levels given by the suppliers. In order to reduce the amount of volatile impurities, all samples were dried for at least 48 h under vacuum (10^{-3} Pa) at room temperature, before use. After the drying procedure, the water content of each sample was determined using a Metrohm 831 Karl Fisher coulometer with an associated uncertainty of ±3 μg. The water content was found to be less than 290 ppm for all ILs. The analyte used for the coulometric Karl Fisher titration was Hydranal-Coulomat AG from Riedel-de Haën. In all experiments, water was double distilled, passed by a reverse osmosis system and further treated with a Milli-Q plus 185 water purification apparatus.

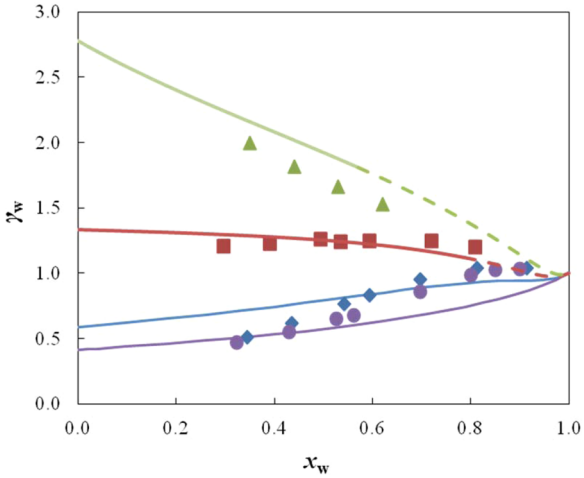

Figure 1. Experimental and predicted water activity coefficients, at 298.2 K. Symbols are representing experimental data and full lines the COSMO-RS predictions (violet line and ●) [BMIM][DCA], (blue line and ◆) [BMIM][SCN], (red line and ■) [BMIM][TCM] and (green line and ▲) [EMIM][TCB]. The dashed lines for [BMIM]-[TCM] and [EMIM][TCB] indicate the immiscibility region of these ILs in water.

2.2. Water Activity Measurements. A Novasina hygrometer LabMaster-a_w (Switzerland) was used to measure water activities, a_w. The measuring principle of the instrument is based on resistive-electrolytic method. The accuracy of the instrument is 0.001 a_w, enabling measurements under controlled chamber temperature conditions (±0.15 K), and was previously calibrated with six saturated pure salt standard solutions, with a_w ranging from 0.330 to 0.973, which were included in the instrument. Prior to the measurement, a calibration curve was built using KCl or $CaCl_2$ aqueous solutions at different salt molalities, depending on the water activity range values to be measured. The obtained values were compared to those recommended in the extensive reviews by Archer[40] for KCl, or Rard and Clegg[41] for $CaCl_2$. For each

DOI: 10.1021/jp510125x
J. Phys. Chem. B 2015, 119, 1567−1578

measurement, samples ca. 2−3 cm^3 were prepared gravimetrically with uncertainties of ±0.0001 g in the entire range of solubility of ILs. The samples were then charged in the measuring cells and placed in the airtight equilibrium chamber. The exchange of free water took place until the partial pressure of water vapor reached the equilibrium, which was confirmed following the a_w variation with time. The value of water activity was recorded when it reached a constant value. For solutions with high concentration of IL, times of up to 8 h were required for constant water activity. At the end, the mole fractions were confirmed by measuring the refractive index (five measurements were performed for each mixture), using an automated Abbemat 500 Anton Paar refractometer. Those were carried out at the temperature 298.15 K for all samples, at atmospheric pressure. The maximum deviation in temperature is ±0.01 K and the maximum uncertainty in the refractive index measurements is ±0.00002. The water activity coefficients, γ_w, were estimated according to the following equation,

$$\gamma_w = \frac{a_w}{x_w} \tag{1}$$

where a_w is the water activity and x_w the water mole fraction.

3. THEORETICAL METHODS

3.1. COSMO-RS. The COSMO-RS approach proposed by Klamt and Schuurmann,[42] is a unique method for *a priori* prediction of the phase behavior of pure fluids and their mixtures on the basis of unimolecular quantum chemical calculations. A comprehensive description of the COSMO-RS theory can be found at the original work of Klamt et al.[43] An important advantage of COSMO-RS model is that it can be used to predict the activity coefficient of any component in a mixture without using any experimental information. It uses the molecular structure of the solute/component as single initial input. Thus, it can be used to predict the water activity coefficients in aqueous binary mixtures containing ILs. The reliability of COSMO-RS to predict the activity coefficient of a solute in ILs has been shown by us[19,20] and others.[44,45] Therefore, in this work, COSMO-RS was used to predict water activity coefficients in the binary mixtures with CN-based ILs and to further understand the water-ILs interactions.

The standard procedure on using COSMO-RS to predict activity coefficients consists of two main steps. In the first step, continuum solvation COSMO calculations of electronic density and molecular geometry were performed with the TURBOMOLE 6.5 package[46] at the BP-TZVPD-FINE level,[47] introduced in 2012. It is based on a Turbomole BP-RI-DFT COSMO single point calculation with TZVPD basis set on top of an optimized BP/TZVP/COSMO geometry. The COSMO single point calculation considers the TZVPD basis set, TZVP with diffuse functions, and a novel type of molecular surface cavity construction (fine grid marching tetrahedron cavity, FINE[48]) which creates a COSMO surface whose segments are more uniform and evenly distributed compared to the standard COSMO cavity. Calculations at the same levels of theory are also performed at the gas phase. In the second step, the estimation of the water activity coefficient data for each binary mixture was performed with the COSMOtherm program using the parameter file BP_TZVPD-FINE_C30_0140 (COSMOlogic GmbH & Co KG, Leverkusen, Germany).[47] In all calculations, the interaction energies of the surface pairs are defined in terms of the screening charge densities σ and σ' of the respective surface segments, with the resulting information being stored in the so-called COSMO files. Subsequently, the chemical potential (μ_s) of a surface segment (σ), the so-called sigma potential (σ - potential) is calculated using the following equation,

$$\mu_s(\sigma) = -\frac{RT}{a_{\text{eff}}} \ln\left[\int p_s(\sigma') \exp\left\{\frac{a_{\text{eff}}}{RT}[\mu_S(\sigma') - E_{\text{misfit}}(\sigma, \sigma') - E_{\text{HB}}(\sigma, \sigma')]\right\} d\sigma'\right] \tag{2}$$

where a_{eff} represents the effective contact area, $p_s(\sigma)$ stands for the surface screening charge distribution of the whole system, E_{misfit} is the electrostatic misfit energy, E_{HB} is the hydrogen-bonding energy, R is the ideal gas constant and T the absolute temperature. The chemical potential of a compound is available from the integration of the σ-potential over the surface of the molecule, and it is used for the prediction of thermodynamic properties and phase behavior, as it is used on the prediction of the water activity coefficients in systems with ILs using the equation below,[45]

$$\gamma_s^{X_i} = \exp\left\{\frac{\mu_S^{X_i} - \mu_{X_i}^{X_i}}{RT}\right\} \tag{3}$$

where $\gamma_S^{X_i}$ is the activity coefficient of compound X_i in the solvent S, $\mu_S^{X_i}$ is its chemical potential in the solvent S and $\mu_{X_i}^{X_i}$ is the chemical potential of pure compound X_i. In this work, the ILs were always treated as isolated ions at the quantum chemical level.

Another advantage of using COSMO-RS, is that it can also provide other thermodynamic properties to get further insight toward the interaction of water and ILs. For example, the excess enthalpies can be used to infer on the strength of water-ILs interaction in the binary mixture. The excess enthalpy is defined as the difference between the interaction of IL and water in their mixture and pure state, according to eq 4,

$$H^E = H_{i,mixture} - H_{i,pure} \tag{4}$$

The predicted excess enthalpies can be further analyzed according to the contribution of specific interaction of cation, anion and water molecule, according to eqs 5−8,

$$H^E = H^E_{cation} + H^E_{anion} + H^E_{water} \tag{5}$$

The total excess enthalpy in the COSMO-RS method arises from summing the three specific interactions, namely electrostatic-misfit, H^E_{MF}, hydrogen bonds, H^E_{HB}, and van der Waals forces, H^E_{vdW}. Thereafter, each term of eq 5 can then be written as following,

$$H^E_{cation} = H^E_{MF,cation} + H^E_{HB,cation} + H^E_{vdW,cation} \tag{6}$$

$$H^E_{anion} = H^E_{MF,anion} + H^E_{HB,anion} + H^E_{vdW,anion} \tag{7}$$

$$H^E_{water} = H^E_{MF,water} + H^E_{HB,water} + H^E_{vdW,water} \tag{8}$$

Therefore, COSMO-RS allows the evaluation of the energetic contributions of all possible specific interactions established by each species and their contributions to the total excess enthalpy, as well as, their mechanisms of interaction.

3.2. Molecular Dynamics Simulations. Molecular dynamics simulations were performed with the GROMACS[49] code, version 4.5.4, for binary aqueous systems, at IL mole

DOI: 10.1021/jp510125x
J. Phys. Chem. B 2015, 119, 1567−1578

fractions of 0.2, 0.4, 0.6, and 0.8, for the following ILs: [BMIM][SCN], [BMIM][DCA], [BMIM][TCM], and [EMIM][TCB]. Further details on the number of molecules in each system are provided in Table S1 in the Supporting Information.

For all the systems, after energy minimization and equilibration runs, production runs of 20 ns within the isothermal−isobaric (*NPT*) ensemble were performed using a time step of 2 fs. In these simulations, the temperature was maintained constant at 298.15 K using the Nosé−Hoover[50,51] thermostat, and the pressure was kept at 1 bar with the Parrinello−Rahman[52] barostat. The intermolecular interaction energy between pairs of neighboring atoms was calculated using the Lennard-Jones potential to describe dispersion/repulsion forces and the point-charge Coulomb potential was used for electrostatic forces. Cut-offs of 1.2 and 1.0 nm were set for Lennard-Jones and Coulombic interactions, respectively, and long-range corrections for energy and pressure were also applied. Rigid constraints were enforced on all bonds lengths. Additionally, for each system, simulations within the canonical ensemble (*NVT*) were also performed for 10 ns, under the same conditions as those considered in the *NPT* simulations.

The force field parameters for the $[BMIM]^+$ cation were taken from Cadena and Maginn,[53] while those for the $[EMIM]^+$ cation were deduced from the former. The potential parameters for the $[SCN]^-$ anion were those used in our previous work,[54] for the $[DCA]^-$ and $[TCM]^-$ anions were considered the OPLS-AA force field[55,56] parameters, while those for the $[TCB]^-$ anion were obtained from the work of Koller et al.[57] The atomic charges for the IL cations and anions were recalculated in the present work with the CHelpG scheme[58] using an optimized geometry (minimum energy from several configurations) for each IL ion pair, in the gaseous phase as performed previously for other systems involving ILs.[54,59] The calculations were performed at the B3LYP/6-311+G(d) level of theory[60] with the Gaussian 09 code.[61] The total charges on the cations and anions were ±0.804 *e* for [BMIM][SCN], ± 0.826 *e* for [BMIM][DCA], ± 0.880 *e* for [BMIM][TCM] and ±0.889 *e* for [EMIM][TCB]. The full sets of atomic charges for each IL are compiled in Tables S2 to S5 in the Supporting Information. Water molecules considered the SPCE model.[62] To validate the combination of the different force fields applied for each cation and anion, densities for each pure IL were estimated, at 298.15 K, and are compared with the experimental values recently published by Neves et al.[26] in Table S6 in the Supporting Information. A very satisfactory agreement between experimental and simulated data is observed with relative deviations of 3.2%, 1.8%, 1.6% and 1.2% in the cases of [BMIM][DCA], [EMIM][TCB], [BMIM][TCM], and [BMIM][SCN], respectively.

In addition, radial and spatial distributions functions, RDFs and SDFs, respectively, as well as coordination numbers, *Z*, were calculated from the MD trajectories.

4. RESULTS AND DISCUSSION

4.1. Water Activities and Activity Coefficients. The experimental water activities together with the respective water activity coefficients, calculated using eq 1, are given in Table 1. Figure 1 presents a comparison of experimental and COSMO-RS water activity coefficients of the ILs. The water activity coefficients of ([BMIM][SCN] + water) and ([BMIM][DCA] + water) binary mixtures present up to x_w = 0.8 values lower than unit, which indicates favorable interactions between [BMIM][SCN] or [BMIM][DCA] and water molecules. On the other hand, unfavorable interactions between [BMIM][TCM] and [EMIM][TCB] with water are observed, being their water activity coefficients higher than unit throughout whole composition. It should be stressed that high and positive values of water activity coefficients in [EMIM][TCB] and [BMIM][TCM] eventually lead to the formation of two phases, as observed experimentally.[63] In the case of [BMIM][TCM] the formation of phases occurs at high water content, x_w = 0.80, while for [EMIM][TCB] the phenomenon occurs already at x_w = 0.60. For this reason the experimental data were carefully measured within the region of complete miscibility for these ILs. Accordingly, based on the strength of their interactions with water, the studied cyano-based ILs can be ranked in the order [EMIM][TCB] < [BMIM][TCM] < BMIM][SCN] < [BMIM][DCA].

Table 1. Experimental Water Activities (a_w) and Experimental and COSMO-RS Water Activity Coefficients (γ_w) in the Binary Mixtures at T = 298.2 K

x_w	a_w	$\gamma_{w,exp}$	$\gamma_{w,COSMO}$	ARD, %[a]
		[BMIM][SCN] + H_2O		
0.436	0.269	0.617	0.761	23.2
0.541	0.413	0.763	0.812	6.5
0.594	0.492	0.829	0.839	1.1
0.696	0.664	0.954	0.888	6.9
0.812	0.842	1.037	0.931	10.2
0.914	0.948	1.038	0.945	9.0
0.956	0.970	1.015	0.952	6.2
			AAD[b]	9.0
		[BMIM][DCA] + H_2O		
0.323	0.151	0.467	0.505	8.0
0.429	0.235	0.548	0.544	0.7
0.526	0.341	0.648	0.586	9.7
0.561	0.381	0.679	0.602	11.3
0.697	0.596	0.856	0.679	20.6
0.800	0.788	0.985	0.754	23.5
0.849	0.869	1.023	0.796	22.2
0.899	0.929	1.034	0.846	18.1
			AAD[b]	14.3
		[BMIM][TCM] + H_2O		
0.296	0.357	1.204	1.294	7.5
0.390	0.478	1.227	1.278	4.2
0.493	0.620	1.257	1.254	0.2
0.534	0.662	1.241	1.243	0.2
0.593	0.740	1.248	1.223	2.0
0.720	0.896	1.245	1.165	6.4
0.808	0.970	1.201	1.106	7.9
			AAD[b]	4.1
		[EMIM][TCB] + H_2O		
0.350	0.698	1.994	2.158	8.2
0.440	0.799	1.816	2.017	11.1
0.530	0.881	1.662	1.875	12.8
0.620	0.948	1.529	1.725	12.8
			AAD[b]	11.2

[a]Average relative deviation between experimental and COSMO-RS water activity coefficients. [b]Average absolute deviation between experimental and COSMO-RS water activity coefficients.

4.2. COSMO-RS Calculations. From the results shown in Figure 1, it is evident that the COSMO-RS model predicts qualitatively the water activity coefficients of the studied CN-based ILs, with average absolute deviations (AAD) varying

DOI: 10.1021/jp510125x
J. Phys. Chem. B 2015, 119, 1567−1578

between 4.1% for [BMIM][TCM] and 14.3% for [BMIM]-[DCA]. It should be pointed out that in a previous work,[19] we used an older version of COSMO-RS parametrization TZVP_C30_1301 to predict the water activity coefficients in binary mixtures with [BMIM][SCN]. The newer parametrization produces, however, lower relative deviations, showing a significant improvement in the quality of predicted results. The associated BP_TZVPD_FINE_C30_0140.ctd parameter set, used in this work, additionally incorporates the HB2012 hydrogen bonding term and a novel van der Waals dispersion term based on the "D3" method of Grimme et al.[64] These lead to improved thermodynamic property predictions for compound classes where the previous COSMO-RS hydrogen bonding term showed weaknesses. In addition, COSMO-RS correctly predicts the experimentally observed trend of CN-based ILs interactions with water. Thus, in the following discussion, COSMO-RS is also used to probe the interactions of ILs and water.

Figure 2 (and S2 in the Supporting Information) depicts the σ-profiles and σ–potentials for water and the four ILs (for each

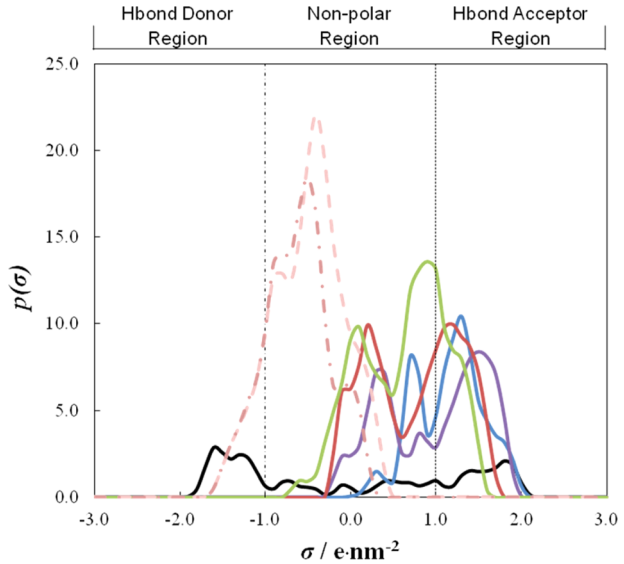

Figure 2. σ profiles for (black line) water, (violet line) $[DCA]^-$, (blue line) $[SCN]^-$, (red line) $[TCM]^-$, (green line) $[TCB]^-$, (light pink dashed line) $[BMIM]^+$, and (dark pink dashed–dotted line) $[EMIM]^+$.

anion and cation) addressed in this study. The σ-profiles are obtained by converting the 3D distribution of the screening charge density into a surface composition function, which can be used to understand the behavior of the molecule in terms of its polarity.

The σ–potentials, obtained from eq 2, describe the affinities of molecules to interact with molecules of the same kind. The two vertical dotted lines in Figure 2, are the locations of the cut off values for the H-bond donor ($\sigma_{HB} < -1.0$ e·nm^{-2}) and acceptor ($\sigma_{HB} > 1.0$ e·nm^{-2}) profiles. For instance, the σ-profile of water is very broad, spanning throughout negative, positive, and neutral areas from −2.0 to +2.1 e·nm^{-2} because of the expected behavior for water to act as H-bond donor or acceptor. On the negative area, the peak at −1.6 e·nm^{-2} is assigned to the two polar hydrogen atoms of water, indicating the ability of this molecule to act as H-bond donor. On the positive side, broad peaks centered at 1.8 e·nm^{-2} resulting from the two pairs of electrons belonging to the oxygen atom of the water molecule. This peak designates the ability of water to act also as H-bond acceptor through its oxygen atom. Hence, water can act either as H-bond donor or H-bond acceptor, depending on the behavior of the other molecule in the mixture. Consequently, as displayed by its σ–potential, water presents considerable attraction to both H-bond donors and H-bond acceptors.

Regarding the studied ILs, asymmetries on both σ-profiles and σ-potentials are observed, certainly due to an uneven charge distribution along the ILs' structure. The ILs' cations present a shoulder-like peak at −0.9 e·nm^{-2}, close to the cut off, attributed to the acidic hydrogen atom in the imidazolium ring that could act as a weak H-bond donor. Meanwhile, the anions present a peak within the positive area indicating their potential as H-bond acceptors. The weak H-bond donor ability of the IL cation is surpassed by the high H-bond acceptor characteristics of the anions, and the studied CN-based ILs as a whole present enhanced interactions with other molecules displaying H-bond donor features, as depicted by their σ–potentials.

It is interesting to observe the shifting of the anion peaks into the positive region. Going from $[SCN]^-$ to $[DCA]^-$, the peak moves to a more positive area, indicating that the latter anion is more electronegative.[43] This shifting is indicative of a stronger ability of $[DCA]^-$ to act as H-bond acceptor when compared to the $[SCN]^-$ anion. Interestingly, further increasing the number of CN groups into the anion, as in the cases of $[TCM]^-$ and $[TCB]^-$, significantly shifts the peak toward the neutral area, with the latter anion shifting the most. Thus, it indicates that, while increasing the number of CN groups from thiocyanate to dicyanamide the H-bond acceptor character is increased, a further increase of the number of CN groups from dicyanamide to tetracyanoborate decreases their abilities to act as H-bond acceptor. As a consequence, it is expected that $[DCA]^-$ will have the strongest interaction with water, followed by $[SCN]^-$, $[TCM]^-$, and at last $[TCB]^-$.

Afterward, the contributions of the electrostatic misfit, hydrogen bonding, and van der Waals interactions to the total excess enthalpy of IL and water at equimolar composition, $x_w = 0.5$, estimated through eqs 5–8, are depicted in Figure 3.

Negative total excess enthalpies are observed for the aqueous binary mixtures of [BMIM][SCN] or [BMIM][DCA], where electrostatic misfit interactions and hydrogen bonding are the main contributions for the exothermic process, while positive total excess enthalpies (endothermic processes) are found for aqueous binary mixtures of [BMIM][TCM] and [EMIM]-[TCB]. The results demonstrate that the hydrogen bonding between anion and water plays a crucial role and determines the enthalpic nature of the mixtures, albeit the electrostatic misfit has a minor contribution to exothermicity of the mixture, while the van der Waals contribution is always found to be positive. The combination of all these contributions leads to the following behavior with the increase of the number of CN groups in the anion: from thiocyanate to dicyanamide the total excess enthalpies become more negative while from the latter anion to tetracyanoborate, the sign of the total excess enthalpy is reversed and becomes more positive. In other words, the hydrogen bonding becomes weaker with increasing number of CN groups in the anion, which is in close agreement with the extended series of hydrogen bonding basicity taken from the solvatochromic parameter.[65] The solvatochromic parameter β, measures the hydrogen-accepting ability of an ion/compound, and it was measured for several ILs.[26,66−69] In a recent work

DOI: 10.1021/jp510125x
J. Phys. Chem. B 2015, 119, 1567−1578

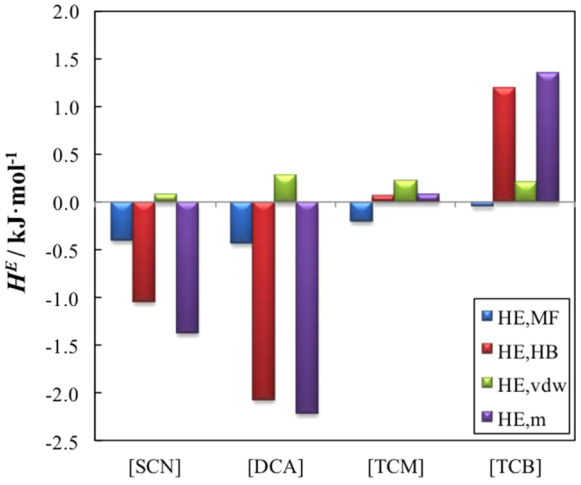

Figure 3. Contribution of specific interaction to the total excess enthalpy, at x_w = 0.5 and T = 298.15 K. The contribution of excess enthalpies from electrostatic/misfit is represented by the blue bars, hydrogen bonding through the red bars, van der Waals through the green bars, and total excess enthalpies of the mixtures by the violet bars.

from our group,[65] it was possible to estimate the solvatochromic parameter β for the studied ILs which are, 0.671, 0.762, 0.666, and 0.598 for [BMIM][SCN], [BMIM][DCA], [BMIM][TCM] and [EMIM][TCB], respectively, suggesting that the ability to establish H-bonds increases from [BMIM][SCN] to [BMIM][DCA], and afterward it decreases with an increase of the CN groups in the anion.

4.3. Molecular Dynamics Simulations. *4.3.1. Radial Distribution Functions and Coordination Numbers.* Radial distribution function, $g(r)$ or RDF, gives the probability of finding a particle at the distance r, from another particle (considered as the reference) and will be here used to describe the local structural organization of the mixtures studied in this work. The RDF values provide a quantitative description of enhancement (values above than one) or depletion (values below than one) of densities of atoms, or groups of atoms, around a selected moiety with respect to bulk values. Moreover, the local environment around the reference atom can be accurately represented by the coordination number (Z), which is the average number of atoms of one type surrounding the reference atom within a cut off, r_Z, given by the integral of RDF.

$$Z(r) = 4 \times \pi \times \rho_B \times \int_0^{r_z} (r^2 g(r))\, dt \tag{9}$$

The cutoff is usually chosen to be the first local minimum of the corresponding RDF. Figures 4 and 5 present the RDFs and Table 2 compiles the coordination numbers obtained for all systems under study. The analyses of the anion-solvent, cation-

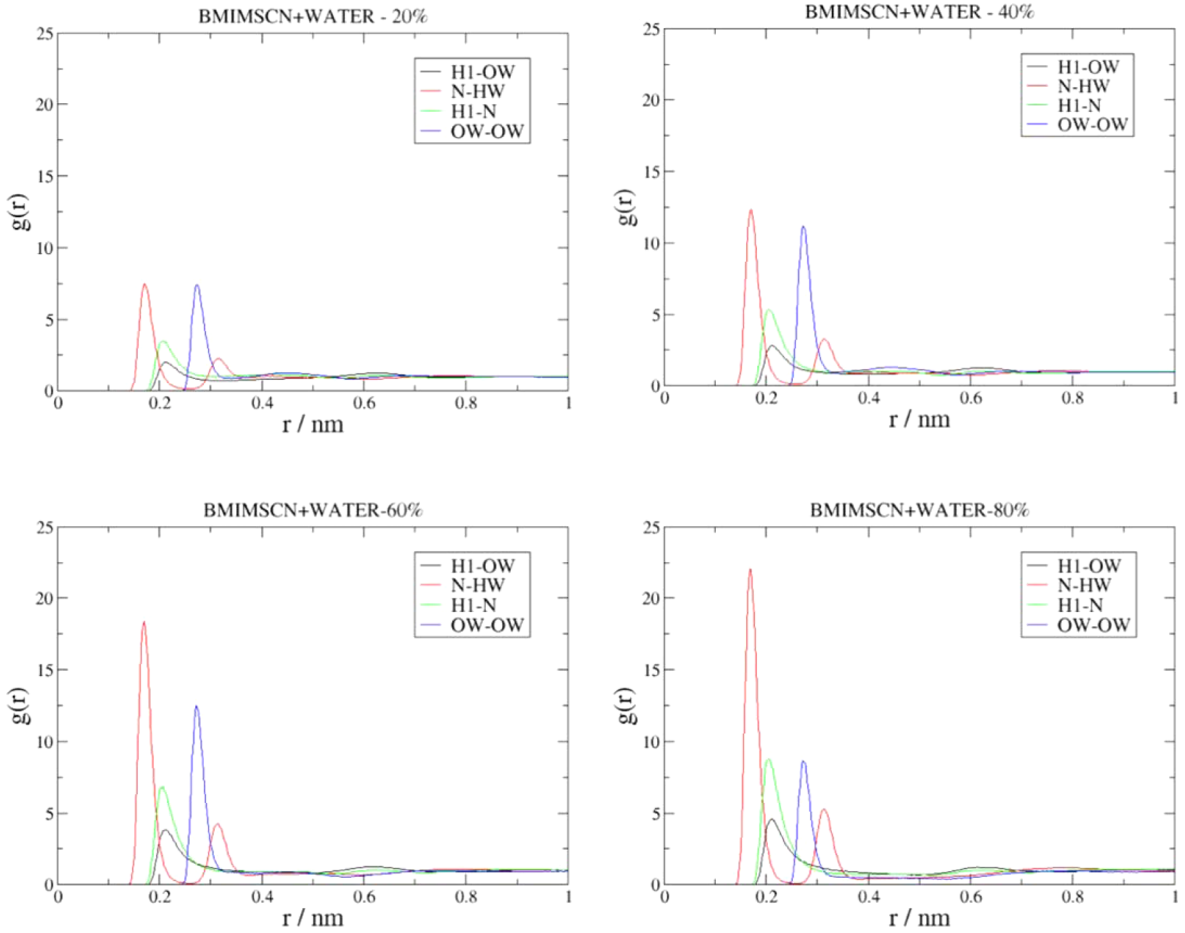

Figure 4. Radial distributions functions (RDFs) for mixtures of [BMIM][SCN] and water, at different mole fractions of IL and 298.15 K. RDFs for interaction of cation-water (H1−OW, black line), anion−water (N−HW, red line), cation−anion (H1−N, green line), and solvent−solvent (OW−OW, blue line) are represented in each panel.

DOI: 10.1021/jp510125x
J. Phys. Chem. B 2015, 119, 1567−1578

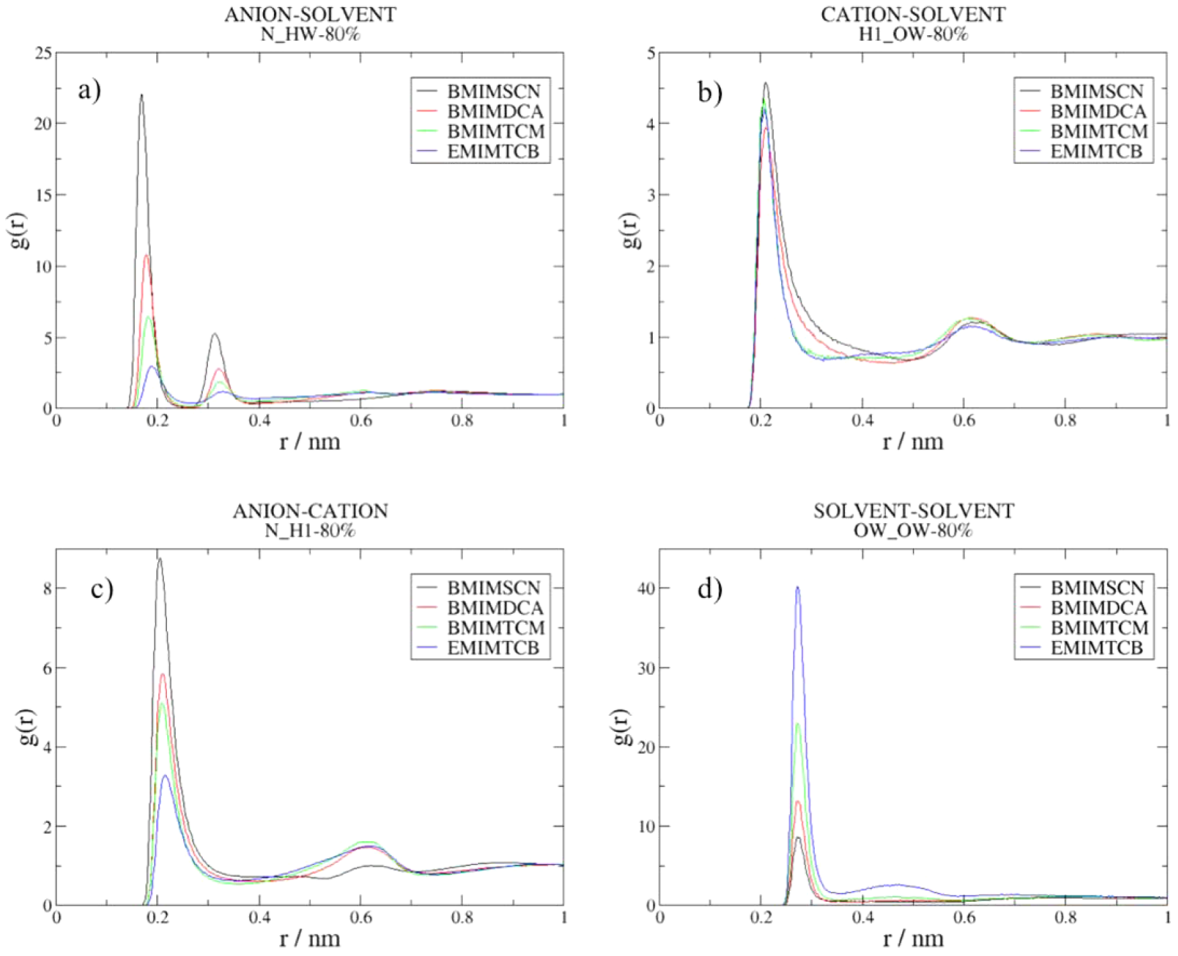

Figure 5. Radial distributions functions (RDFs) for a) anion-water, b) cation-water, c) cation−anion and d) water−water interactions, at 80IL:20W and 298.15 K. RDFs for [BMIM][SCN] (black line), [BMIM][DCA] (red line), [BMIM][TCM] (green line), and [EMIM][TCB] (blue line) are represented in each panel.

solvent, cation−anion and solvent−solvent interactions are based on the RDFs obtained for the N−HW, H1−OW, H1−N, and OW−OW pairs, respectively, where N is the nitrogen atom of the cyano group(s) in the anion, H1 is the acidic proton of the cation, and HW and OW stand for proton and oxygen atoms in water.

Common to all IL systems and similar to what was inferred from the COSMO-RS σ-profiles, the RDFs in Figures 4 and 5, and Figures S3−S5 in the Supporting Information, show that the primary interaction with water occurs with the anion, through N-HW atoms, while cation-water interactions are observed at the next solvation shell, suggesting that the latter is weaker than the former interaction. Moreover, as expected, interactions established among water molecules also present high values of $g(r)$. The latter interactions seem to be competing with anion-water interactions, being observed that water−water interactions are predominant in the case of [EMIM][TCB], for all composition range (see Figure S8 in Supporting Information). In general, all these interactions are enhanced as the content of IL increases in the mixture, which is in agreement with published studies[1] and suggests the formation of water aggregates.

Notice that we performed MD simulations for the systems of water with [BMIM][TCM] and [EMIM][TCB] starting from random configurations and in the time lengths of the simulations phase separation was not observed. For that reason, RDFs and Z values for the system [EMIM][TCB] and water at 20% of IL's content are also reported.

The RDFs presented can give us additional information concerning the establishment of hydrogen bonds in a mixture. In concordance with the geometric criteria, in the case of water−water interactions, it is recognized formation of a H-bond when a site-to-site RDF O−O (or O−H) presents a first minimum (r_z) in a distance smaller than 0.35 nm (or 0.26 nm) along with an angle of 30°.[70]

In our systems, the primary interactions are anion-water contacts that are mediated through the nitrogen atoms from the IL's anion with the water's hydrogen atoms. The r_z for all considered systems, for this type of interaction, was found to be 0.26 nm, which is consistent with the establishment of a H-bond. For water−water interactions, 0.35 nm was also found to be the r_z for O−O site-to-site RDFs, confirming the establishment of H-bonds. In Figure 5a) are shown the RDFs corresponding to anion-water interactions, for all systems addressed, with IL molar percentage of 80%. The cyano group in the system with the anion $[SCN]^-$ presents higher probability of being surrounded by water than the cyano groups in the other anions, and the RDF presents two well-defined peaks suggesting the presence of two solvation shells. The shapes of the RDFs corresponding to the anion-water interactions are similar but the heights of the peaks decrease from systems having the $[SCN]^-$ anion to $[DCA]^-$ to $[TCM]^-$

DOI: 10.1021/jp510125x
J. Phys. Chem. B 2015, 119, 1567−1578

Table 2. Coordination Number (Z) from the RDF Peaks at Distance Below r_Z nm for Anion−Solvent, Cation−Solvent, Cation−Anion, and Solvent−Solvent Interaction, at Each Considered System and Different IL Mole Fraction

	[BMIM][SCN] + H_2O								
	anion−solvent		cation-solvent		cation−anion		solvent−solvent		IL−solvent
x_{IL}	r_Z	Z	r_Z	Z	r_Z	Z	r_Z	Z	Z (total)
0.2	0.26	2.0	0.40	2.1	0.35	0.5	0.34	2.6	4.1
0.4	0.26	1.4	0.40	1.2	0.35	0.8	0.34	1.7	2.6
0.6	0.26	0.9	0.40	0.7	0.35	1.0	0.34	0.9	1.6
0.8	0.26	0.4	0.40	0.3	0.35	1.1	0.34	0.2	0.7
	[BMIM][DCA] + H_2O								
	anion−solvent		cation−solvent		cation−anion		solvent−solvent		IL−solvent
x_{IL}	r_Z	Z	r_Z	Z	r_Z	Z	r_Z	Z	Z (total)
0.2	0.26	3.2	0.40	2.2	0.35	0.8	0.34	2.4	5.4
0.4	0.26	1.9	0.40	1.2	0.35	1.2	0.34	1.3	3.1
0.6	0.26	1.1	0.40	0.6	0.35	1.4	0.34	0.7	1.7
0.8	0.26	0.5	0.40	0.2	0.35	1.5	0.34	0.3	0.7
	[BMIM][TCM] + H_2O								
	anion−solvent		cation−solvent		cation−anion		solvent−solvent		IL−solvent
x_{IL}	r_Z	Z	r_Z	Z	r_Z	Z	r_Z	Z	Z (total)
0.2	0.26	3.4	0.40	2.0	0.35	1.0	0.34	2.3	5.4
0.4	0.26	1.9	0.40	1.0	0.35	1.4	0.34	1.4	2.9
0.6	0.26	1.0	0.40	0.5	0.35	1.6	0.34	0.8	1.5
0.8	0.26	0.4	0.40	0.2	0.35	1.7	0.34	0.5	0.6
	[EMIM][TCB] + H_2O								
	anion−solvent		cation−solvent		cation−anion		solvent−solvent		IL−solvent
x_{IL}	r_Z	Z	r_Z	Z	r_Z	Z	r_Z	Z	Z (total)
0.2	0.26	3.0	0.40	1.7	0.35	1.4	0.34	2.7	4.7
0.4	0.26	1.6	0.40	0.8	0.35	1.8	0.34	2.0	2.4
0.6	0.26	0.9	0.40	0.4	0.35	1.9	0.34	1.4	1.3
0.8	0.26	0.4	0.40	0.2	0.35	2.1	0.34	0.9	0.6

and, finally, to $[TCB]^-$. This trend is the opposite of that verified for water−water interactions in the four systems considered, cf. Figure 5d), suggesting that segregation of water decreases in the following order $[TCB]^- > [TCM]^- > [DCA]^- > [SCN]^-$. In the case of the cation-solvent interactions, cf. Figure 5b), all ILs have similar interactions with water, though the RDF for [BMIM][SCN] is slightly more pronounced than the corresponding interaction in the other studied ILs. Plots similar to those displayed in Figure 5, for IL mole fractions of 20%, 40% and 60% are provided in the Supporting Information (Figures S6−S8), and trends are identical to those described for the 80% solutions. An exception, however, can be found in the ordering for the cation−solvent interactions, where [BMIM]-[TCM] presents higher probability of interaction with water. For further analyses, the mixture composed by 80% of IL and 20% of water, on a molar basis, will be referred to as 80IL:20W.

Additional information regarding the interactions involved in the ILs−water solutions can be obtained from the coordination numbers that are reported in Table 2. These numbers allow to quantify the number of H-bonds that are established between the species, by taking into account not only the heights of the first peaks in the RDFs, but also their widths and the densities of the different systems. Apparent discrepancies with the analyses of the heights of the RDF peaks result from differences in the number of cyano groups in the anions and also from differences in the density of each composition as a consequence of different contents of each compound.

Results in Table 2 demonstrate that the largest values concerning the IL-water interactions, i.e., obtained by adding the cation-water and anion-water interactions in all range of composition, are found for the system with the anion $[DCA]^-$, suggesting more favorable interactions with water, which is in close agreement with the experimental findings from the present study. At 20% and 40% of IL, $[DCA]^-$ is followed by (or is nearly equal to) the system with the anion $[TCM]^-$, then by $[TCB]^-$ and finally by $[SCN]^-$. This trend is not obtained, however, for 60% and 80% of IL, where it is found that the IL-water coordination numbers for the system with the anion $[DCA]^-$ are still the largest but the ordering of the remaining systems is different; i.e., the second largest is the system composed by $[SCN]^-$, then $[TCM]^-$, and finally $[TCB]^-$. The latter ordering is the same as that obtained for the experimental water activity coefficient data and for the COSMO-RS predictions. The Z values for cation−anion interactions are increasing with the content of IL in the system, contrary to the trends observed for the interactions with water. Regarding water−water interactions, they decrease less dramatically with the content of IL from the system containing the anion $[SCN]^-$, through $[DCA]^-$, $[TCM]^-$, and $[TCB]^-$. As mentioned previously, this trend is accompanied by an increase of cation−anion interactions, suggesting that the systems are gradually losing the propensity to interact with water as the number of CN groups increase in the IL's anion.

Similar to what was discussed previously, the capacity of these ILs to establish H-bonds can be supported by the

DOI: 10.1021/jp510125x
J. Phys. Chem. B 2015, 119, 1567−1578

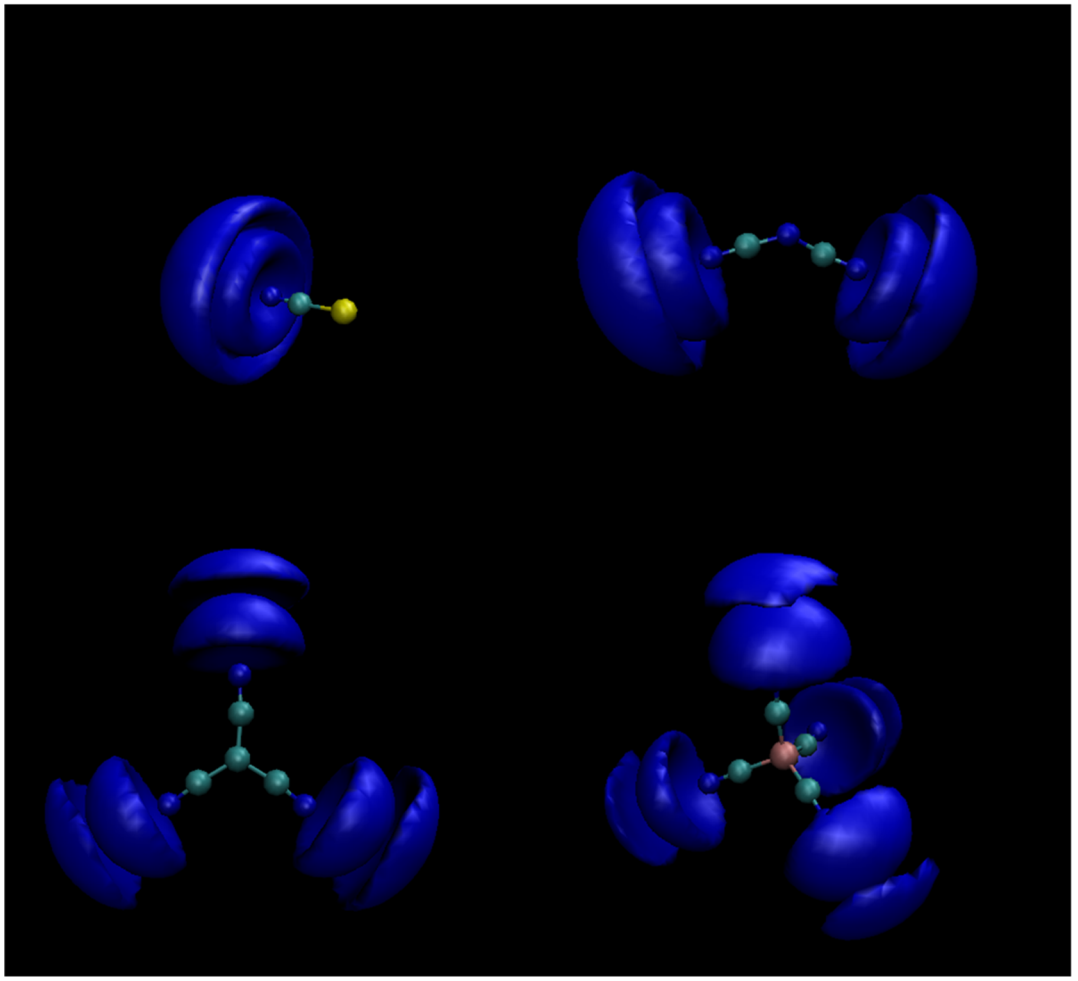

Figure 6. Spatial distribution functions (SDFs) obtained by TRAVIS,[72] for the mixture [BMIM][SCN] (above, left side), [BMIM][DCA] (above, right side), [BMIM][TCM] (down, left side) and [EMIM][TCB] (down, right side) and water, at 80IL:20W. Each anion is the central element, surrounded by oxygen atoms of water (blue surface).

solvatochromic parameter β. Moreover, the CHelpG charges calculated at the B3LYP/6-311+G(d) level of theory can also give us some insights regarding the obtained results. Aiming this, and since results have demonstrated that the anions are the mediators of the interactions with water through their nitrogen atoms, atomic charges for all nitrogen atoms in the cyano groups of the anions are reported in Tables S2−S5. As it can be observed, charges of the nitrogen atoms become less negative in the order $[DCA]^-$ > $[SCN]^-$ > $[TCM]^-$ > $[TCB]^-$ with values of −0.723 *e*, −0.658 *e*, −0.638 *e*, and −0.487 *e*. Notice that the ordering of the partial charges in the nitrogen atoms of the cyano group differ slightly from the ordering of the total charge in the anions which becomes less negative in the order $[SCN]^-$ > $[DCA]^-$ > $[TCM]^-$ > $[TCB]^-$.

The differences found in the partial atomic charges of the cyano nitrogen atoms are due to the presence of different central atoms in each anion, i.e., sulfur ($[SCN]^-$), nitrogen ($[DCA]^-$), carbon ($[TCM]^-$) and boron ($[TCB]^-$), which lead to different charge delocalization. Such differences confer different abilities of the anions to establish H-bonds with water molecules with consequences in the properties of the ILs, for instance, in the anomalous behavior of viscosity.[30] Interestingly, the ordering of the partial charges in the nitrogen atoms from the CN groups in the anions of the ILs agrees with the ordering of the experimental and predicted water activity coefficients. Nevertheless, it is unquestionable that MD simulations allowed to recognize that an increase of CN groups on ILs' anion hinders the ability of these CN-based ILs to interact favorably with water, generally in the same order as observed from water activity coefficient data.

4.3.2. Solvent Accessible Surface Area and Spatial Distribution Functions. Aiming at a tridimensional visualization of how each anion interacts with water; i.e., the most important interaction type on these systems, the solvent accessible surface areas (*sasa*, the surface area of one molecule that is accessible to a solvent) and the spatial distribution functions (SDFs, a 3D representation of the probability of finding a particle at a certain position) were calculated for solutions 80IL:20W. The *sasa* surfaces were obtained as Connolly surfaces[71] consisting of all points at which a solvent sphere can reach based on the van der Waals radii. Figure S9 in the Supporting Information shows the *sasa* surfaces for each anion under study. The nodes are represented as atoms and the vertices joining the nearest nodes as connect records. Results demonstrate that water connects preferentially to all nitrogen atoms that are sterically available, becoming a specific interaction in the case of $[SCN]^-$.

The SDFs were built and analyzed with the TRAVIS[72] utility considering isosurfaces with values of 6.56 particles·nm^{-3} for the $[BMIM]^+$ and $[EMIM]^+$ cations (red surfaces, Figure S10

DOI: 10.1021/jp510125x
J. Phys. Chem. B 2015, 119, 1567−1578

in Supporting Information) and of 1.24 particles·nm^{-3} for water (blue surfaces, Figure 6 and Figure S10 in Supporting Information), around the ILs anions in solutions 80IL:20W. As a common characteristic to all ILs, and in agreement to what was observed above in the analysis of the RDFs, water molecules preferentially interact with the nitrogen atoms of the cyano groups from the anions. Moreover, SDFs for the anion−water interaction clearly show the existence of two solvation shells (Figure 6). The SDFs for the anion−water and cation−anion interactions (Figure S10 in the Supporting Information) suggest a competition between water molecules and cations for the anions since regions concerning the two interaction types are found at similar distances. Furthermore, in the cases of the $[SCN]^-$ and $[DCA]^-$ anions, the SDFs for the cation−anion interactions (Figure S10) show that the cations not only interact with nitrogen atoms from CN groups but also with the sulfur atom of $[SCN]^-$ and with the core of $[DCA]^-$. Additionally, the volume of the SDFs for water interacting with the different anions (Figure 6) decrease with the increase of the hydrophobicity of the anion, suggesting that the interaction is more likely in the case of the anions with less CN groups, which is consistent with conclusions arising from all the other analyses developed in this work.

5. CONCLUSIONS

Aiming to study water−ILs interaction, aqueous solutions of [BMIM][SCN], [BMIM][DCA], [BMIM][TCM], and [EMIM][TCB] were studied and characterized by means of experimental and computational techniques.

Experimental water activity and the corresponding water activity coefficients suggest that [BMIM][SCN], [BMIM]-[DCA] are able to establish favorable interactions with water molecules as given by the negative deviations to ideality. On the contrary, [BMIM][TCM] and [EMIM][TCB] present positive deviations to ideality, indicating nonfavorable or weak interactions with water. Moreover, COSMO-RS is shown to be able to quantitatively predict the water activity coefficients, presenting average absolute deviations varying from 4.1 to 14.3% for the aqueous systems with [BMIM][TCM] and [BMIM][DCA], respectively. According to sigma profile, generated using COSMO-RS, the electronegativity of the anions plays a crucial role toward their interaction with water molecules. The increasing of the number of CN groups from $[SCN]^-$ to $[DCA]^-$, slightly increases the electronegativity, improving interactions with water molecules. However, increasing the number of CN groups from $[DCA]^-$ to $[TCB]^-$ it is observed a decrease of the electronegativity, as well as their ability to act as H-bond acceptors.

Information at the atomic level was retrieved from DFT calculated partial atomic charges, and from the analyses of RDFs, coordination numbers, SDFs and *sasa* surfaces based on the trajectories obtained from MD simulation. They support the trend of IL-water and water−water interactions inferred from the activity coefficients results. According to the partial atomic charges, not only it was possible to infer that the anions establish important interactions with water through the nitrogen atoms of the CN groups but also that the central atom has a deterministic impact on the charge delocalization of the anion. Because of the latter factor, together with the increasing number of CN groups, the propensity of interaction with water decreases. Additionally, due to the high ionic interaction between cation and anion, the cations seem to establish some important H-bond contacts with water molecules that should not be neglected, though they seem to be have less effect than those involving the anions. Hence, the propensity for formation of ILs aggregates is expected to be smaller in the case of [BMIM][SCN] and [BMIM][DCA].

In general, the information retrieved from the experimental and computational results shows that the anion governs the interaction between ILs and water. The increase of the number of CN groups in the ILs' anion from thiocyanate to dicyanamide is accompanied by an increase in the ability of the anion to establish H-bonds with water, while from dicyanamide to tricyanomethanide to tetracyanoborate it is found that the H-bond propensity decreases.

■ ASSOCIATED CONTENT

Supporting Information

Tables containing atomic charges and figures representing σ profile, radial and spatial distribution functions, and *sasa*s, and a complete ref 61. This material is available free of charge via the Internet at http://pubs.acs.org.

■ AUTHOR INFORMATION

Corresponding Author

*(J.A.P.C.) Telephone: +351-234-370200; Fax: +351-234-370084; E-mail address: jcoutinho@ua.pt.

Notes

The authors declare no competing financial interest.

■ ACKNOWLEDGMENTS

This work was financed by Fundação para a Ciência e a Tecnologia (FCT, Portugal), European Union, QREN, FEDER and COMPETE for funding the CICECO (project PEst-C/CTM/LA0011/2013), and LSRE/LCM (project PEst-C/EQB/LA0020/2013) and for Programa Investigador FCT. FCT is also acknowledged for the Ph.D. and Postdoctoral Grants SFRH/BD/74551/2010 and SFRH/BPD/88101/2012 for M.L.S.B. and K.A.K., respectively.

■ REFERENCES

(1) Kirchner, B. *Topics in Current Chemistry*; De Meijere, V. B. A., Kessler, K. N. H. H., Ley, J. L. S. V., Schreiber, M. O. S., Vogel, B. M. T. P., Wong, F. V. H., Eds.; Springer: Germany, 2009; p. Vol. *290*.

(2) Bhattacharjee, A.; Varanda, C.; Freire, M. G.; Matted, S.; Santos, L. M. N. B. F.; Marrucho, I. M.; Coutinho, J. A. P. Density and Viscosity Data for Binary Mixtures of 1-Alkyl-3-Methylimidazolium Alkylsulfates + Water. *J. Chem. Eng. Data* **2012**, *57*, 3473−3482.

(3) Carvalho, P. J.; Regueira, T.; Santos, L. M. N. B. F.; Fernandez, J.; Coutinho, J. A. P. Effect of Water on the Viscosities and Densities of 1-Butyl-3-Methylimidazolium Dicyanamide and 1-Butyl-3-Methylimidazolium Tricyanomethane at Atmospheric Pressure. *J. Chem. Eng. Data* **2009**, *55*, 645−652.

(4) Almeida, H. F. D.; Lopes-da-Silva, J. A.; Freire, M. G.; Coutinho, J. A. P. Surface Tension and Refractive Index of Pure and Water-Saturated Tetradecyltrihexylphosphonium-Based Ionic Liquids. *J. Chem. Thermodyn.* **2013**, *57*, 372−379.

(5) Niazi, A. A.; Rabideau, B. D.; Ismail, A. E. Effects of Water Concentration on the Structural and Diffusion Properties of Imidazolium-Based Ionic Liquid-Water Mixtures. *J. Phys. Chem. B* **2013**, *117*, 1378−1388.

(6) Kurnia, K. A.; Pinho, S. P.; Coutinho, J. A. P. Evaluation of the Conductor-like Screening Model for Real Solvents for the Prediction of the Water Activity Coefficient at Infinite Dilution in Ionic Liquids. *Ind. Eng. Chem. Res.* **2014**, *53*, 12466−12475.

(7) Pereiro, A. B.; Araújo, J. M. M.; Esperança, J. M. S. S.; Marrucho, I. M.; Rebelo, L. P. N. Ionic Liquids in Separations of Azeotropic Systems − A Review. *J. Chem. Thermodyn.* **2012**, *46*, 2−28.

DOI: 10.1021/jp510125x
J. Phys. Chem. B 2015, 119, 1567−1578

(8) Zakrzewska, M. E.; Bogel-Lukasik, E.; Bogel-Lukasik, R. Solubility of Carbohydrates in Ionic Liquids. *Energy Fuels* **2010**, *24*, 737−745.
(9) Cammarata, L.; Kazarian, S. G.; Salter, P. A.; Welton, T. Molecular States of Water in Room Temperature Ionic Liquids. *Phys. Chem. Chem. Phys.* **2001**, *3*, 5192−5200.
(10) Fumino, K.; Wulf, A.; Ludwig, R. Hydrogen Bonding in Protic Ionic Liquids: Reminiscent of Water. *Angew. Chem., Int. Ed. Engl.* **2009**, *48*, 3184−3186.
(11) Freire, M. G.; Neves, C. M. S. S.; Silva, A. M. S.; Santos, L. M. N. B. F.; Marrucho, I. M.; Rebelo, L. P. N.; Shah, J. K.; Maginn, E. J.; Coutinho, J. A. P. (1)H NMR and Molecular Dynamics Evidence for an Unexpected Interaction on the Origin of Salting-In/Salting-Out Phenomena. *J. Phys. Chem. B* **2010**, *114*, 2004−2014.
(12) Singh, T.; Kumar, A. Aggregation Behavior of Ionic Liquids in Aqueous Solutions: Effect of Alkyl Chain Length, Cations, and Anions. *J. Phys. Chem. B* **2007**, *111*, 7843−7851.
(13) Królikowska, M. (Solid+liquid) and (liquid+liquid) Phase Equilibria of (IL+water) Binary Systems. The Influence of the Ionic Liquid Structure on Mutual Solubility. *Fluid Phase Equilib.* **2014**, *361*, 273−281.
(14) Królikowska, M.; Karpińska, M.; Zawadzki, M. Phase Equilibria Study of the Binary Systems (N-Hexylisoquinolinium Thiocyanate Ionic Liquid + Organic Solvent or Water). *J. Phys. Chem. B* **2012**, *116*, 4292−4299.
(15) Królikowska, M.; Zawadzki, M.; Królikowski, M. Physicochemical and Thermodynamic Study on Aqueous Solutions of Dicyanamide − Based Ionic Liquids. *J. Chem. Thermodyn.* **2014**, *70*, 127−137.
(16) Passos, H.; Khan, I.; Mutelet, F.; Oliveira, M. B.; Carvalho, P. J.; Santos, L. M. N. B. F.; Held, C.; Sadowski, G.; Freire, M. G.; Coutinho, J. A. P. Vapor-Liquid Equilibria of Water + Alkylimidazolium-Based Ionic Liquids: Measurements and Perturbed-Chain Statistical Associating Fluid Theory Modeling. *Ind. Eng. Chem. Res.* **2014**, 3737−3748.
(17) Domańska, U.; Krolikowski, M.; Paduszynski, K. Phase Equilibria Study of the Binary Systems (N-Butyl-3-Methylpyridinium Tosylate Ionic Liquid plus an Alcohol). *J. Chem. Thermodyn.* **2009**, *41*, 932−938.
(18) Domańska, U.; Marciniak, A.; Królikowska, M.; Arasimowicz, M. Activity Coefficients at Infinite Dilution Measurements for Organic Solutes and Water in the Ionic Liquid 1-Hexyl-3-Methylimidazolium Thiocyanate. *J. Chem. Eng. Data* **2010**, *55*, 2532−2536.
(19) Khan, I.; Kurnia, K. A.; Mutelet, F.; Pinho, S. P.; Coutinho, J. A. P. Probing the Interactions between Ionic Liquids and Water: Experimental and Quantum Chemical Approach. *J. Phys. Chem. B* **2014**, 1848−1860.
(20) Khan, I.; Kurnia, K. A.; Sintra, T. E.; Saraiva, J. A.; Pinho, S. P.; Coutinho, J. A. P. Assessing the Activity Coefficients of Water in Cholinium-Based Ionic Liquids: Experimental Measurements and COSMO-RS Modeling. *Fluid Phase Equilib.* **2014**, *361*, 16−22.
(21) Kelkar, M. S.; Maginn, E. J. Effect of Temperature and Water Content on the Shear Viscosity of the Ionic Liquid 1-Ethyl-3-Methylimidazolium Bis(trifluoromethanesulfonyl)imide as Studied by Atomistic Simulations. *J. Phys. Chem. B* **2007**, *111*, 4867−4876.
(22) Chevrot, G.; Schurhammer, R.; Wipff, G. Molecular Dynamics Simulations of the Aqueous Interface with the [BMI][PF6] Ionic Liquid: Comparison of Different Solvent Models. *Phys. Chem. Chem. Phys.* **2006**, *8*, 4166−4174.
(23) Hanke, C. G.; Lynden-Bell, R. M. A Simulation Study of Water−Dialkylimidazolium Ionic Liquid Mixtures. *J. Phys. Chem. B* **2003**, *107*, 10873−10878.
(24) Bhargava, B. L.; Yasaka, Y.; Klein, M. L. Computational Studies of Room Temperature Ionic Liquid-Water Mixtures. *Chem. Commun.* **2011**, *47*, 6228−6241.
(25) Zhong, X.; Fan, Z.; Liu, Z.; Cao, D. Local Structure Evolution and Its Connection to Thermodynamic and Transport Properties of 1-Butyl-3-Methylimidazolium Tetrafluoroborate and Water Mixtures by Molecular Dynamics Simulations. *J. Phys. Chem. B* **2012**, *116*, 3249−3263.
(26) Crowhurst, L.; Mawdsley, P. R.; Perez-Arlandis, J. M.; Salter, P. A.; Welton, T. Solvent-Solute Interactions in Ionic Liquids. *Phys. Chem. Chem. Phys.* **2003**, *5*, 2790−2794.
(27) Fumino, K.; Wulf, A.; Ludwig, R. The Potential Role of Hydrogen Bonding in Aprotic and Protic Ionic Liquids. *Phys. Chem. Chem. Phys.* **2009**, *11*, 8790−8794.
(28) Canongia Lopes, J. N.; Costa Gomes, M. F.; Pádua, A. A. H. Nonpolar, Polar, and Associating Solutes in Ionic Liquids. *J. Phys. Chem. B* **2006**, *110*, 16816−16818.
(29) Dommert, F.; Wendler, K.; Berger, R.; Delle Site, L.; Holm, C. Force Fields for Studying the Structure and Dynamics of Ionic Liquids: A Critical Review of Recent Developments. *ChemPhysChem* **2012**, *13*, 1625−1637.
(30) Neves, C. M. S. S.; Kurnia, K. A.; Coutinho, J. A. P.; Marrucho, I. M.; Lopes, J. N. C.; Freire, M. G.; Rebelo, L. P. N. Systematic Study of the Thermophysical Properties of Imidazolium-Based Ionic Liquids with Cyano-Functionalized Anions. *J. Phys. Chem. B* **2013**, *117*, 10271−10283.
(31) Zhou, D.; Bai, Y.; Zhang, J.; Cai, N.; Su, M.; Wang, Y.; Zhang, M.; Wang, P. Anion Effects in Organic Dye-Sensitized Mesoscopic Solar Cells with Ionic Liquid Electrolytes: Tetracyanoborate vs Dicyanamide. *J. Phys. Chem. C* **2011**, *115*, 816−822.
(32) Marszalek, M.; Fei, Z.; Zhu, D.-R.; Scopelliti, R.; Dyson, P. J.; Zakeeruddin, S. M.; Grätzel, M. Application of Ionic Liquids Containing Tricyanomethanide $[C(CN)3]^-$ or Tetracyanoborate $[B(CN)4]^-$ Anions in Dye-Sensitized Solar Cells. *Inorg. Chem.* **2011**, *50*, 11561−11567.
(33) Heitmann, S.; Krings, J.; Kreis, P.; Lennert, A.; Pitner, W. R.; Górak, A.; Schulte, M. M. Recovery of N-Butanol Using Ionic Liquid-Based Pervaporation Membranes. *Sep. Purif. Technol.* **2012**, *97*, 108−114.
(34) Meindersma, G. W.; Hansmeier, A. R.; de Haan, A. B. Ionic Liquids for Aromatics Extraction. Present Status and Future Outlook. *Ind. Eng. Chem. Res.* **2010**, *49*, 7530−7540.
(35) Cláudio, A. F. M.; Freire, M. G.; Freire, C. S. R.; Silvestre, A. J. D.; Coutinho, J. A. P. Extraction of Vanillin Using Ionic-Liquid-Based Aqueous Two-Phase Systems. *Sep. Purif. Technol.* **2010**, *75*, 39−47.
(36) Swatloski, R. P.; Spear, S. K.; Holbrey, J. D.; Rogers, R. D. Dissolution of Cellose with Ionic Liquids. *J. Am. Chem. Soc.* **2002**, *124*, 4974−4975.
(37) Zhao, H.; Baker, G. A.; Song, Z.; Olubajo, O.; Crittle, T.; Peters, D. Designing Enzyme-Compatible Ionic Liquids That Can Dissolve Carbohydrates. *Green Chem.* **2008**, *10*, 696−705.
(38) Conceiçao, L. J. A.; Bogel-Łukasik, E.; Bogel-Łukasik, R. A New Outlook on Solubility of Carbohydrates and Sugar Alcohols in Ionic Liquids. *RSC Adv.* **2012**, *2*, 1846−1855.
(39) Kurnia, K. A.; Coutinho, J. A. P. Overview of the Excess Enthalpies of the Binary Mixtures Composed of Molecular Solvents and Ionic Liquids and Their Modeling Using COSMO-RS. *Ind. Eng. Chem. Res.* **2013**, *52*, 13862−13874.
(40) Archer, D. G. Thermodynamic Properties of the KCl+H2O System. *J. Phys. Chem. Ref. Data* **1999**, *28*, 1−17.
(41) Rard, J. A.; Clegg, S. L. Critical Evaluation of the Thermodynamic Properties of Aqueous Calcium Chloride. 1. Osmotic and Activity Coefficients of 0−10.77 $Mol{\cdot}kg^{-1}$ Aqueous Calcium Chloride Solutions at 298.15 K and Correlation with Extended Pitzer Ion-Interaction Models. *J. Chem. Eng. Data* **1997**, *42*, 819−849.
(42) Klamt, A.; Schuurmann, G. COSMO: A New Approach to Dielectric Screening in Solvents with Explicit Expressions for the Screening Energy and Its Gradient. *J. Chem. Soc. Perkin Trans. 2* **1993**, 799−805.
(43) Klamt, A. *COSMO-RS: From Quantum Chemistry to Fluid Phase Thermodynamics and Drug Design*; Elsevier: Amsterdam, 2005.
(44) Reddy, P.; Aslam Siddiqi, M.; Atakan, B.; Diedenhofen, M.; Ramjugernath, D. Activity Coefficients at Infinite Dilution of Organic Solutes in the Ionic Liquid PEG-5 Cocomonium Methylsulfate at T=(313.15, 323.15, 333.15, and 343.15)K: Experimental Results and COSMO-RS Predictions. *J. Chem. Thermodyn.* **2013**, *58*, 322−329.

DOI: 10.1021/jp510125x
J. Phys. Chem. B 2015, 119, 1567−1578

(45) Diedenhofen, M.; Eckert, F.; Klamt, A. Prediction of Infinite Dilution Activity Coefficients of Organic Compounds in Ionic Liquids Using COSMO-RS. *J. Chem. Eng. Data* **2003**, *48*, 475−479.
(46) Furche, F.; Ahlrichs, R.; Hättig, C.; Klopper, W.; Sierka, M.; Weigend, F. Turbomole. *Wiley Interdiscip. Rev. Comput. Mol. Sci.* **2014**, *4*, 91−100.
(47) Eckert, F.; Klamt, A. COSMOtherm Version C3.0 Release 14.01, 2013.
(48) Klamt, A.; Reinisch, J.; Eckert, F.; Graton, J.; Le Questel, J.-Y. Interpretation of Experimental Hydrogen-Bond Enthalpies and Entropies from COSMO Polarisation Charge Densities. *Phys. Chem. Chem. Phys.* **2013**, *15*, 7147−7154.
(49) Hess, B.; Kutzner, C.; van der Spoel, D.; Lindahl, E. GROMACS 4: Algorithms for Highly Efficient, Load-Balanced, and Scalable Molecular Simulation. *J. Chem. Theory Comput.* **2008**, *4*, 435−447.
(50) Nose, S. A Molecular-Dynamics Method For Simulations in the Canonical Ensemble. *Mol. Phys.* **1984**, *52*, 255−268.
(51) Hoover, W. G. Canonical Dynamics - Equilibrium Phase-Space Distributions. *Phys. Rev. A* **1985**, *31*, 1695−1697.
(52) Parrinello, M.; Rahman, A. Polymorphic Transitions in Single-Crystals - A New Molecular-Dynamics Method. *J. Appl. Phys.* **1981**, *52*, 7182−7190.
(53) Cadena, C.; Maginn, E. J. Molecular Simulation Study of Some Thermophysical and Transport Properties of Triazolium-Based Ionic Liquids. *J. Phys. Chem. B* **2006**, *110*, 18026−18039.
(54) Batista, M. L. S.; Tomé, L. I. N.; Neves, C. M. S. S.; Rocha, E.; Gomes, J. R. B.; Coutinho, J. A. P. The Origin of the LCST on the Liquid-Liquid Equilibrium of Thiophene with Ionic Liquids. *J. Phys. Chem. B* **2012**, *116*, 5985−5992.
(55) Jorgensen, W. L.; Maxwell, D. S.; Tirado-Rives, J. Development and Testing of the OPLS All-Atom Force Field on Conformational Energetics and Properties of Organic Liquids. *J. Am. Chem. Soc.* **1996**, *118*, 11225−11236.
(56) Kaminski, G. A.; Friesner, R. A.; Tirado-Rives, J.; Jorgensen, W. L. Evaluation and Reparametrization of the OPLS-AA Force Field for Proteins via Comparison with Accurate Quantum Chemical Calculations on Peptides †. *J. Phys. Chem. B* **2001**, *105*, 6474−6487.
(57) Koller, T.; Ramos, J.; Garrido, N. M.; Fröba, A. P.; Economou, I. G. Development of a United-Atom Force Field for 1-Ethyl-3-Methylimidazolium Tetracyanoborate Ionic Liquid. *Mol. Phys.* **2012**, *110*, 1115−1126.
(58) Breneman, C. M.; Wiberg, K. B. Determining Atom-Centered Monopoles from Molecular Electrostatic Potentials. The Need for High Sampling Density in Formamide Conformational Analysis. *J. Comput. Chem.* **1990**, *11*, 361−373.
(59) Batista, M. L. S.; Coutinho, J. A. P.; Gomes, J. R. B. Prediction of Ionic Liquids Properties through Molecular Dynamics Simulations | BenthamScience. *Curr. Phys. Chem.* **2014**, *4*, 151−172.
(60) Becke, A. D. Density-Functional Thermochemistry. III. The Role of Exact Exchange. *J. Chem. Phys.* **1993**, *98*, 5648−5652.
(61) Frisch, M. J. .; Trucks, G. W. .; Schlegel, H. B. .; Scuseria, G. E. .; Robb, M. A. .; Cheeseman, J. R. .; Scalmani, G. .; Barone, V. .; Mennucci, B. .; Petersson, G. A. .; et al. *Gaussian 09, Revision D.01*; Gaussian, Inc.: Wallingford CT, 2009.
(62) Berendsen, H. J. C.; Grigera, J. R.; Straatsma, T. P. The Missing Term in Effective Pair Potentials. *J. Phys. Chem.* **1987**, *91*, 6269−6271.
(63) Freire, M. G.; Neves, C.; Carvalho, P. J.; Gardas, R. L.; Fernandes, A. M.; Marrucho, I. M.; Santos, L.; Coutinho, J. A. P. Mutual Solubilities of Water and Hydrophobic Ionic Liquids. *J. Phys. Chem. B* **2007**, *111*, 13082−13089.
(64) Grimme, S.; Antony, J.; Ehrlich, S.; Krieg, H. A Consistent and Accurate Ab Initio Parametrization of Density Functional Dispersion Correction (DFT-D) for the 94 Elements H-Pu. *J. Chem. Phys.* **2010**, *132*, 154104−154123.
(65) Cláudio, A. F.; Swift, L.; Hallett, J.; Welton, T.; Coutinho, J. A. P.; Freire, M. G. Extended Scale for the Hydrogen-Bond Basicity of Ionic Liquids. *Phys. Chem. Chem. Phys.* **2014**, *16*, 6593−6601.
(66) Lungwitz, R.; Spange, S. A Hydrogen Bond Accepting (HBA) Scale for Anions, Including Room Temperature Ionic Liquids. *New J. Chem.* **2008**, *32*, 392−394.
(67) Lungwitz, R.; Strehmel, V.; Spange, S. The Dipolarity/polarisability of 1-Alkyl-3-Methylimidazolium Ionic Liquids as Function of Anion Structure and the Alkyl Chain Length. *New J. Chem.* **2010**, *34*, 1135−1140.
(68) Lungwitz, R.; Friedrich, M.; Linert, W.; Spange, S. New Aspects on the Hydrogen Bond Donor (HBD) Strength of 1-Butyl-3-Methylimidazolium Room Temperature Ionic Liquids. *New J. Chem.* **2008**, *32*, 1493−1499.
(69) Ab Rani, M. A.; Brant, A.; Crowhurst, L.; Dolan, A.; Lui, M.; Hassan, N. H.; Hallett, J. P.; Hunt, P. A.; Niedermeyer, H.; Perez-Arlandis, J. M.; et al. Understanding the Polarity of Ionic Liquids. *Phys. Chem. Chem. Phys.* **2011**, *13*, 16831−16840.
(70) Skarmoutsos, I.; Dellis, D.; Matthews, R. P.; Welton, T.; Hunt, P. A. Hydrogen Bonding in 1-Butyl- and 1-Ethyl-3-Methylimidazolium Chloride Ionic Liquids. *J. Phys. Chem. B* **2012**, *116*, 4921−4933.
(71) Connolly, M. L. Analytical Molecular Surface Calculation. *J. Appl. Crystallogr.* **1983**, *16*, 548−558.
(72) Brehm, M.; Kirchner, B. TRAVIS - a Free Analyzer and Visualizer for Monte Carlo and Molecular Dynamics Trajectories. *J. Chem. Inf. Model.* **2011**, *51*, 2007−2023.

DOI: 10.1021/jp510125x
J. Phys. Chem. B 2015, 119, 1567−1578